ISSN 1674-1056
http://cpb.iphy.ac.cn
http://iopscience.iop.org/cpb
中国物理 B
Chinese Physics
中国物理 Chinese Physics B

Insulator-metal transition in $CaTiO_3$ quantum dots induced by ultrafast laser pulses

Tong Liu(刘彤), Hong Zhang(张红), Xin-Lu Cheng(程新路)

Citation: Chin. Phys. B . 2020, 29(5): 058101 . **doi:** 10.1088/1674-1056/ab7d9e
Journal homepage: http://cpb.iphy.ac.cn; http://iopscience.iop.org/cpb

What follows is a list of articles you may be interested in

InP quantum dots-based electroluminescent devices

Qianqian Wu(吴倩倩), Fan Cao(曹璠), Lingmei Kong(孔令媚), Xuyong Yang(杨绪勇)

Chin. Phys. B . 2019, 28(11): 118103 . **doi:** 10.1088/1674-1056/ab4cdb

Silica encapsulated ZnO quantum dot-phosphor nanocomposites: Sol-gel preparation and white light-emitting device application

Ya-Chuan Liang(梁亚川), Kai-Kai Liu(刘凯凯), Ying-Jie Lu(卢英杰), Qi Zhao(赵琪), Chong-Xin Shan(单崇新)

Chin. Phys. B . 2018, 27(7): 078102 . **doi:** 10.1088/1674-1056/27/7/078102

Anomalous temperature dependence of photoluminescence spectra from InAs/GaAs quantum dots grown by formation-dissolution-regrowth method

Guan-Qing Yang(杨冠卿), Shi-Zhu Zhang(张世著), Bo Xu(徐波), Yong-Hai Chen(陈涌海), Zhan-Guo Wang(王占国)

Chin. Phys. B . 2017, 26(6): 068103 . **doi:** 10.1088/1674-1056/26/6/068103

Electric-field-dependent charge delocalization from dopant atoms in silicon junctionless nanowire transistor

Hao Wang(王昊), Wei-Hua Han(韩伟华), Xiao-Song Zhao(赵晓松), Wang Zhang(张望), Qi-Feng Lyu(吕奇峰), Liu-Hong Ma(马刘红), Fu-Hua Yang(杨富华)

Chin. Phys. B . 2016, 25(10): 108102 . **doi:** 10.1088/1674-1056/25/10/108102

Enhanced biocompatibility of ZnS:Mn quantum dots encapsulated with *Aloe vera* extract for therapeutic applications

Anilkumar M, Bindu K R, Sneha Saj A, Anila E I

Chin. Phys. B . 2016, 25(8): 088103 . **doi:** 10.1088/1674-1056/25/8/088103

Insulator–metal transition in $CaTiO_3$ quantum dots induced by ultrafast laser pulses*

Tong Liu(刘彤)[1], Hong Zhang(张红)[1,2,†], and Xin-Lu Cheng(程新路)[2]

[1] College of Physics, Sichuan University, Chengdu 610065, China

[2] Key Laboratory of High Energy Density Physics and Technology of Ministry of Education, Sichuan University, Chengdu 610065, China

(Received 15 January 2020; revised manuscript received 18 February 2020; accepted manuscript online 9 March 2020)

According to time-dependent density functional theory (TDDFT), we study the interactions between ultra-fast laser pulses and two kinds of calcium titanate quantum dots (PCTO-QDs and MCTO-QDs). Under the action of localized field effect, ultrafast laser can induce quantum dots to make the transition from insulator to metal. The PCTO-QDs are ultimately metallic, while the MCTO-QDs are still insulator after experiencing metal state. This is bacause the stability of the unsaturated atoms in the outermost layer of PCTO-QDs is weak and the geometric configuration of MCTO-QDs as a potential well will also reduce the damage of laser. Moreover, laser waveforms approaching to the intrinsic frequency of quantum dots tend to cause the highest electron levels to cross the Fermi surface. In this paper, it is reported that the insulating quantum dots can be transformed into metal by adjusting the intensity and frequency of laser. The importance of local morphology is emphasized by comparing two kinds of CTO-QDs. More importantly, it is an important step to identify the potential properties of perovskite materials.

Keywords: ultra-fast laser, $CaTiO_3$ QDs, metallic transformation

PACS: 81.07.Ta, 79.20.Ds, 73.61.–r **DOI:** 10.1088/1674-1056/ab7d9e

1. Introduction

Recently, resurgence of research interest in inorganic perovskite has revealed a promising array of photophysical properties and inspired the development of high-performance photovoltaic cells, light-emitting diodes, and laser technologies.[1–5] Inorganic perovskite quantum dots (QDs) have become a hot research focus because of their excellent characteristics including above-band gap photovoltage, ferroelectric character, and light emission.[6–9] External field effect has been a successful tool to study carrier dynamics in organic semiconductors.[10–12] For example, in many transition metal oxides, the insulator–metal transition has been achieved with external stimuli, including temperature, light, electric field, mechanical strain or magnetic field.[13–15] Energy mediated transfer has been demonstrated by using molecules to couple light into and out of microscale waveguides.[16] Perovskites can form nanoscaled waveguides to generate nanoscaled lasing, which enables perovskite ideal light-emission sources for integrated photonics devices.[17] And the shape-dependent broadband plasmonic effect improves the efficiency of perovskite photovoltaics.[18] All these reveal that the interaction of the laser field with perovskites is a promising research direction with novel photonics applications and the ability to control the properties of perovskites.

Semiconductor quantum dots (QDs) as nanostructures exhibit excellent optical properties due to quantum-size effects, as compared with their bulk structures.[19–21] The results show that the semiconductor QDs have been recognized as an advantageous optical gain material over bulk and quantum well counterparts.[22] In comparison with bulk perovskite films, two-dimensional (2D) perovskite nanosheets with small thickness of a few unit cells are suitable for investigating the intrinsic nonlinear optical properties because bulk recombination of photo-carriers and the nonlinear scattering are relatively small. Electron–electron interactions can render an otherwise conducting material insulating, with the insulator–metal phase transition in correlated-electron materials being the canonical macroscopic manifestation of the competition between charge-carrier itinerancy and localization. The transition can arise from underlying microscopic interactions among the charge, lattice, orbital and spin degrees of freedom, the complexity of the transition leads to multiple phase-transition pathways. Although we have known that the height of quantum dots will affect the bandgap and radiation decay time,[23] the physical property conversion of 2D perovskite quantum dots, especially their application in ultrafast photonics, needs further exploring. Here in this paper, $CaTiO_3$ quantum dots (CTO-QDs), which are a typical perovskite-based metal oxide,[24–26] are selected and investigated in their interaction with ultrafast laser by using the time-dependent density functional theory (TDDFT). By calculating the density of states (DOS) for CTO-QDs with ultrafast laser,

*Project supported by the National Key Research and Development Program of China (Grant No. 2017YFA0303600) and the National Natural Science Foundation of China (Grant Nos. 11974253 and 11774248).

†Corresponding author. E-mail: hongzhang@scu.edu.cn

© 2020 Chinese Physical Society and IOP Publishing Ltd

the highest electron level (HEL) and the number of electrons across the Fermi level (N_F) are evaluated to study the change of the electron occupied states.

In this paper, we mainly explore the interaction between ultrafast laser and CTO-QDs. We design two QDs with different structures for one material CTO, namely PCTO-QDs and MCTO-QDs. The results show that the highest energy electrons can jump and eventually even cross the Fermi surface at the right laser intensity. The physical properties of both QDs are characterized by a shift from insulativity to metallicity. What attract us is the effect in which the final physical properties of the structure under ultrafast laser are directly related to whether or not the QDs are modified. We take a laser with the intensity of 3 eV/Å and the wavelength of 600 nm for example. For the PCTO-QDs, the process of physical property change is an insulation–metal–insulation–metal process. But for the MCTO-QDs, they experience an insulation–metal–insulation process instead. There are many unsaturated atoms at the edges of PCTO-QDs. These atoms are susceptible to permanent damage from lasers field. This causes the metallic nature of the structure to be changed permanently. The laser affects the change of bond length, and also the change of the reaction to DOS, these two changes are also an important reason for the inconsistency of physical properties. In addition, the results show that the laser approaching to the intrinsic frequency of the material can easily adjust the insulation-metal transition. The theoretical calculation results are of great significance for designing and selectingthe QDs in practical experiments.

2. Computational methods

All our calculations are performed by using the real-space and real-time TDDFT code OCTOPUS.[27] The initial point for the time-dependent simulations is solved by the ground-state Kohn-Sham equation. The time-dependent Schrödinger equation to describe photoinduced dynamics is

$$-\mathrm{i}\frac{\partial}{\partial t}\Psi_i(r,t) = \left[-\frac{\nabla^2}{2} + v_{\mathrm{ext}}(r,t) + \mathrm{v}_{\mathrm{hatree}}(n;r,t) + v_{\mathrm{xc}}(n;r,t) + v_{\mathrm{laser}}(r,t)\right]\psi_i(r,t), \quad (1)$$

where $\nabla^2/2$ is the kinetic energy, $v_{\mathrm{ext}}(r,t)$ is the potential of external fields, $v_{\mathrm{hatree}}(n;r,t)$ represents the electron–electron interaction, $v_{\mathrm{xc}}(n;r,t)$ denotes exchange–correlation potential, and $v_{\mathrm{laser}}(r,t)$ describes the classical time-dependent external electromagnetic fields.

The external-fields describe the type and shape of time-dependent external perturbation that are applied to the system, in the form

$$f(x,y,z)\cos(\omega t + \phi(t))g(t), \quad (2)$$

$$g(t) = G_0 \exp[-(t-t_0)^2/2\tau_0^2], \quad (3)$$

where $f(x,y,z)$ is defined by a field type and polarization or a scalar potential, cosine controls the waveform, ω controls the frequency, and $\phi(t)$ is the time-dependent phase. The $g(t)$ function centered around t_0 describes the waveform of the ultrafast laser.

The $CaTiO_3$ quantum dots (CTO-QDs) are described by the Hartwigsen–Goedecker–Hutter pseudopotential. The generalized gradient approximation (GGA) expressed by the Perdew–Burke–Ernzerhof (PBE) functional for the exchange–correlation is used in both the ground-state and excited-state calculations.[28,29] The simulation zone is determined by defining a 6-Å-radius sphere around each atom and a uniform mesh grid of 0.2 Å. For the time evolution, we use a time step of 0.005 $\hbar$/eV $\approx$ 0.0033 fs.

3. Results and discussion

Figures 1(a)–1(d) show the two kinds of CTO-QDs that we designed by an hydroxyl group (MCTO-QDs), namely the pure ones (PCTO-QDs) and the modified ones. Then, we perform the DFT calculations to obtain their ground state by using the optimized configuration for the next excited-state calculations. The two kinds of QDs can converge under the condition of ground state optimization. The structural parameters of length, width and height are also given in Fig. 1.

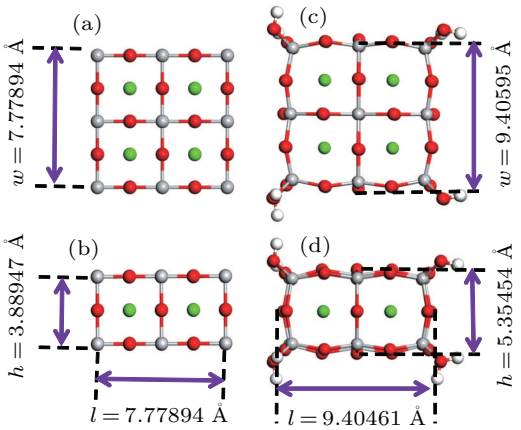


Fig. 1. Top and side view of [(a) and (b)] PCTO-QDs and [(c) and (d)] MCTO-QDs, with l, w, and h representing length, width, and height respectively.

The intrinsic DOS shows that the CTO-QDs are insulating as shown in Fig. 2. The distance from the highest electron level (HEL)s in the two QDs to the Fermi surface are 2.24 eV and 4.78 eV, respectively. The band gap of MCTO-QDs is larger than that of PCTO-QDs, which is because of the atomic position. The studies show that he electronic properties of the materials are strongly influenced by both the sample dimension and boundary condition.[30] We note that the optimized QDs of PCTO and MCTO are different significantly in size and border. Since QDs themselves are on a nanoscale, a tiny

change may lead the fundamental nature of matter to be different radically, and with the atomic position displaced, affected by the quantum size difference, the basic properties of the two QDs are greatly changed.

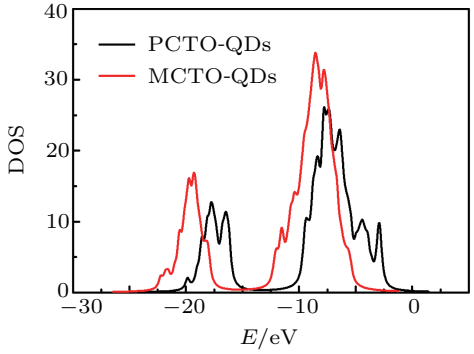


Fig. 2. (a) Intrinsic DOS of CTO-QDs, PCTO-QDs (black), and MCTO-QDs (red).

3.1. Incident ultrafast lasers with different intensities acting on system

Considering the nonnegligible influence of the intensity, we adopt five kinds of incident lasers to study the interaction of ultrafast lasers with CTO-QDs. The intensity of the incident laser ranges from 2.0 eV/Å to 3.0 eV/Å with the intensity interval being 0.25 eV/Å, and the wavelength length being 792 nm as shown in Fig. 3(a). The actual effect of ultra-fast laser is 6 fs. Due to the delay effect of laser,[31] we extend 3 fs to continue observing the interaction between laser and CTO-QDs,

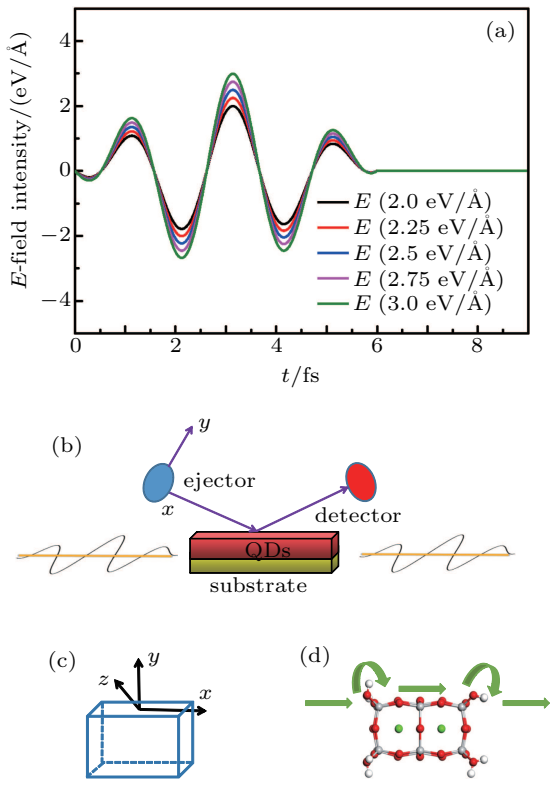


Fig. 3. (a) Laser oscillograph, [(b)–(d)] proposed experimental geometry to illuminate waveguide and laser detector of CTO-QDs equipped with linearly polarized incident laser.

which means that the total duration is 9 fs. Figures 3(b)–3(d) show a proposed experimental model to illuminate the waveguide and laser detector of CTO-QDs equipped with a linearly polarized incident laser. The ultrafast laser goes along the upper surface of the QDs.

3.1.1. HEL and metallicity changing with incident laser

In order to investigate the change of electron occupied state in CTO-QDs under the irradiation of incident ultrafast laser, we first study the time-dependent HELs (see Fig. 4) obtained from DOS. From Fig. 4(a) it can follow that upon the application of the incident ultrafast laser to the HEL, the HEL fluctuation increases (decreases) with electric-field strength increasing (decreasing). For PCTO-QDs (Figs. 4(a) and 4(c)), when the laser intensity is below 2.5 eV, the metallic properties of PCTO-QDs are not changed at all, that is to say, the PCTO-QDs are always in an insulating state. With the gradual increase of laser intensity, the HEL can cross the Fermi surface, at the same time the metallic property of quantum dots realizes the transition from insulation state to metal state. For the MCTO-QDs (Figs. 4(b) and 4(d)), we observe that the HEL is lower than Fermi level under the 2.5 eV/Å intensities, which means that the monolayer CTO nanostructure is still an insulator. When the intensities are 2.75 eV/Å and 3.0 eV/Å, the HEL is higher than the Fermi level, revealing that an insulator–metal transition occurs in the CTO nanostructure. This is because the localized field effect can break the bonds surrounding oxygen atoms, thus thecreating metallic patches to form photocurrents.[12,32]

We take the laser intensity of 3.0 eV/Å for example (Figs. 4(e) and 4(f)). Combining with Fig. 4(a) analysis, when the time of laser incidence reaches 3.55 fs, we find that the HEL continues to vibrate with the laser waveform, but the amplitude of vibration is significantly reduced. The laser action time is totally 6 fs. Considering that the laser has a certain delay effect on the material, the HEL state under laser treatment is also within our research scope. HEL stabilizes over the next 3 fs as the laser disappears. For the PCTO-QDs, HEL is finally higher than the Fermi energy of the surface state. In the whole process from 0 fs to 9 fs, the metallic property of the PCTO-QDs changes from insulator to metal to insulator to metal. That means that the final state ends up with metal. For the MCTO-QDs, HEL with laser waveform is sensitive to change all the time and perfectly fits the shape of the waveform. Within 9 fs, the whole process proceeds from insulator to metal to insulator to metal to insulator. The final state is still of insulator. It suggests that the two types of quantum dots will produce different results when the laser is applied, and their ultimate metallic properties are also determined.

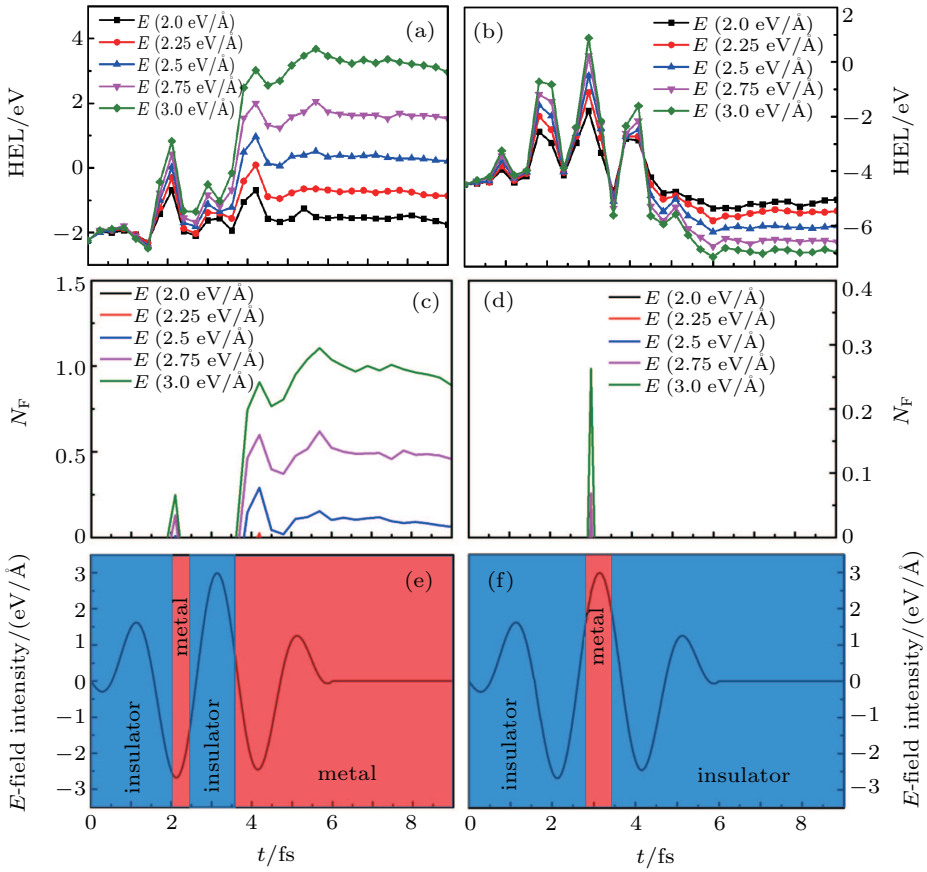


Fig. 4. [(a) and (b)] Highest electron level, [(c) and (d)] electron number across Fermi level (N_F), [(e) and (f)] metallicity of two kinds of QDs varies with laser in 0 fs–9 fs, where [(a), (c), and (e)] and [(b), (d), and (f)] referring to PCTO and MCTO, respectively.

3.1.2. Influence of structural morphology and analysis

Two different results are obtained when the incident laser is applied to two kinds of CTO-QDs. It comes down to three main reasons reasonably. One reason is the difference in structure between the two CTO-QDs themselves. For PCTO-QDs, we need to pay attention to the atoms which are exposed to the outside of the structure. That is to say, these atoms are in an unsaturated state, which means that they are not very stable. In this case, the atoms in the unsaturated state are more sensitive to the efficacy of the laser. After absorbing the laser energy, these electrons outside the atoms are destroyed, thus changing the metallic properties of the PCTO-QDs. By contrast, the outermost atoms of MCTO-QDs are saturated and relatively stable, so its metallic properties are more stable. Figure 5 shows the charge density distribution about two kinds of quantum dots at the different times. Figures 5(a), 5(c), and 5(e) show the laser induced charge density distributions of the PCTO-QDs and figures 5(b), 5(d), and 5(f) exhibit the laser induced charge density distributions of the MCTO-QDs. Obviously, with the ultrafast laser incident, the electrons become active and concentrate after the QDs have absorbed the energy. We focus on the change of edge electron density. Compared with them at time 0 fs, the induced electron density and induced hole density at time 3 fs (Figs. 5(c) and 5(d)) are centralized continuous distribution, indicating that metallic patches are created and an insulator–metal transition occurs. When it comes to 9 fs, we mainly pay attention to the change of edge electron density. Edge electron concentration distribution of PCTO-QDs is obviously different from their initial state. The electrons in PCTO-QDs continue to be concentrated at the edge, which is obviously different from their initial state. We provide the direct evidence that the transformation of metal on CTO-QDs is induced by photoelectric conversion. For MCTO-QDs, the edge electron density is mainly due to modified oxygen atoms and it has no significant change compared with the status at 0 fs. So the initial and final metallic properties are the same. This is another powerful illustration of the ultimate difference in the nature of metal.

The next reason is that for the MCTO-QDs, it is a way to reduce the laser energy by forming a potential well[33,34] because the outermost atoms are saturated and the position of these atoms is slightly higher along the direction of the incident laser. This structure reduces the efficacy of the laser to some extent. In other words, it protects the structure from being damaged by the laser to some extent. As can be seen from Fig. 4, the laser with a strength of 2.5 eV can make the HEL of PCTO-QDs cross the Fermi surface, which, howevev, is not enough to induce the metallic property of MCTO to change. In addition, we also give the sizes of two CTO-QDs under the laser action as shown in Table 1. We can clearly know that the

sizes of QDs vary to different degrees under the laser action. As mentioned above, a small change in quantum dots can exert a huge influence on the properties of the sample.

The last reason can be attributed to the interaction between the laser and structure. We can see that with the change of laser, the structure (length, width, and height) of the two quantum dots vary to different degrees. That is to say, the laser leads to structural changes, and the direct effect on the structure is the change of physical properties. We regard this structural change as structural damage. The change trend of two QDs is inconsistent, that is, with the laser intensity increasing, the length, width, and height of MCTO increase continuously and have an expansion trend. While the length, width, and height of PCTO show an opposite trend. The effect of laser on the structure turns into affecting the physical properties. This reaction is ultimately reflected in the inconsistency of the ultimate metallicity. Therefore, the physical properties of the two trends of structure damage are different. This also provides a reasonable explanation for the inconsistency between the final metal states of the two QDs.

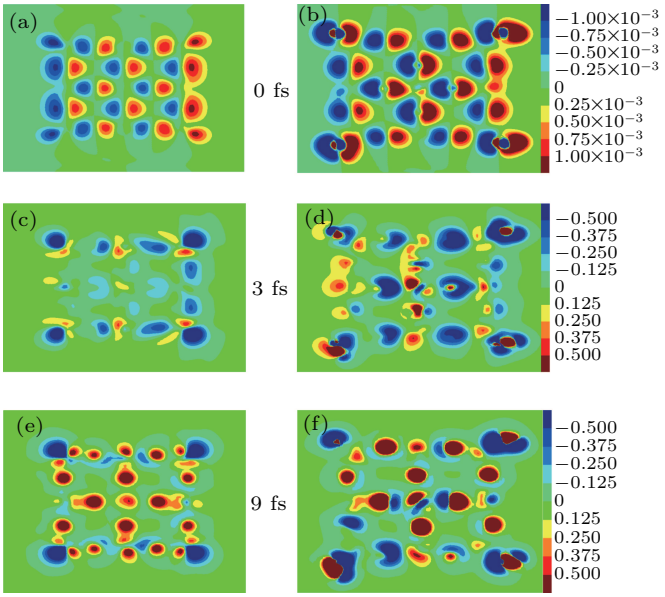


Fig. 5. Laser-induced charge density distribution.

Table 1. Structural changes under different intensities of ultrafast laser.

E-field intensity/eV		2.0	2.25	2.5	2.75	3.0
PCTO-QDs	Δl/%	0.10666	0.10480	0.10317	0.10191	0.10093
	Δw/%	0.11049	0.10968	0.10914	0.10891	0.10913
	Δh/%	0.10029	0.09912	0.09864	0.09810	0.09740
MCTO-QDs	Δl/%	0.738254962	0.749313369	0.763987023	0.77887334	0.795141957
	Δw/%	0.240592391	0.265470261	0.292155497	0.314481791	0.333618614
	Δh/%	0.519932618	0.591834219	0.591834219	0.616859712	0.637776541

3.2. Different wavelength ultrafast lasers incident on system

In the above part, we set the laser wavelength length to be 792 nm, and controlled the laser intensity to observe the metallic property of CTO-QDs. Various wavelength lasers are always used to study optical response properties of materials in various research fields both experimentally and theoretically. The different wavelength lasers can induce different physical properties including superconductivity, magnetic phase transition, and conductivity transition. Therefore, the effects of wavelength are strictly considered in the research of laser–material interactions. In this subsection, we mainly consider the effects of different wavelength lasers on QDs. As shown in Fig. 6, the different wavelength ultrafast lasers ranging from 450 nm to 900 nm, with intensities at 2.5 eV/Å are used to study the interaction of ultrafast laser with CTO-QDs.

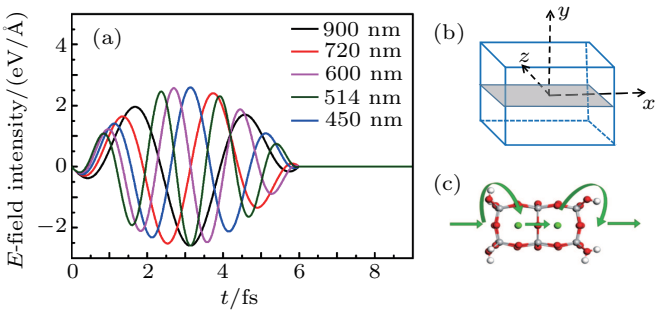


Fig. 6. (a) Different wavelength ultrafast lasers with intensity 2.5 eV/Å, and schematic diagram of (b) QDs placed along *x*–*y* plane and (c) laser incident along *x* direction.

3.2.1. HEL and metallicity changes with incident laser-wave length

As shown in Figs. 7(a) and 7(c), HEL also changes with laser wavelength, which indicates that the insulator–metal transition in CTO-QDs can be induced by controlling the wavelength. Figures 7(b) and 7(d) show that the number of electrons across the Fermi level (N_F) are evaluated to study the change of the electron occupied states. What needs us to pay high attention to is that the changes of two CTO-QDs with wavelength are in the opposite directions. Seemingly, for PCTO-QDs, the longer the wavelength, the more easily the HEL changes to realize the transition from insulator to metallic property. When the wavelengths are 900 nm and 720 nm, the final property of PCTO-QDs is metallic. For the MCTO-QDs, the shorter the wavelength, the the more easily the HEL

changes to cross the Fermi surface. In the case of wavelengths of 450 nm, 514 nm, and 600 nm, the HEL of MCTO-QDs can cross fermi surface, but it is still in an insulating state. It is found that there is no absolute relationship between metallicity and wavelength of the induced laser.

By the way, we note that the laser with a wavelength of 600 nm and a strength of 2.5 eV has a slightly different effect on PCTO mentioned in Subsection 3.1. The energy of laser is not sufficient to metallize the PCTO-QDs (see Fig. 7(b)). In Fig. 4, the laser incident direction is along the upper surface of the quantum dot, while for the laser in Fig. 7, the incident direction is along the center of the quantum dot. In this way, the viewpoint of potential well mentioned at the end of Subsubsection 3.1.2 can also be verified to be correct. When the incident surface is incident along the center, the potential well turns deeper and the more energy is required, so we find it more difficult for the highest electron energy level to cross the Fermi surface. But the trend in HEL is consistent with the laser waveform. This shows that our theoretical calculation results are reliable.

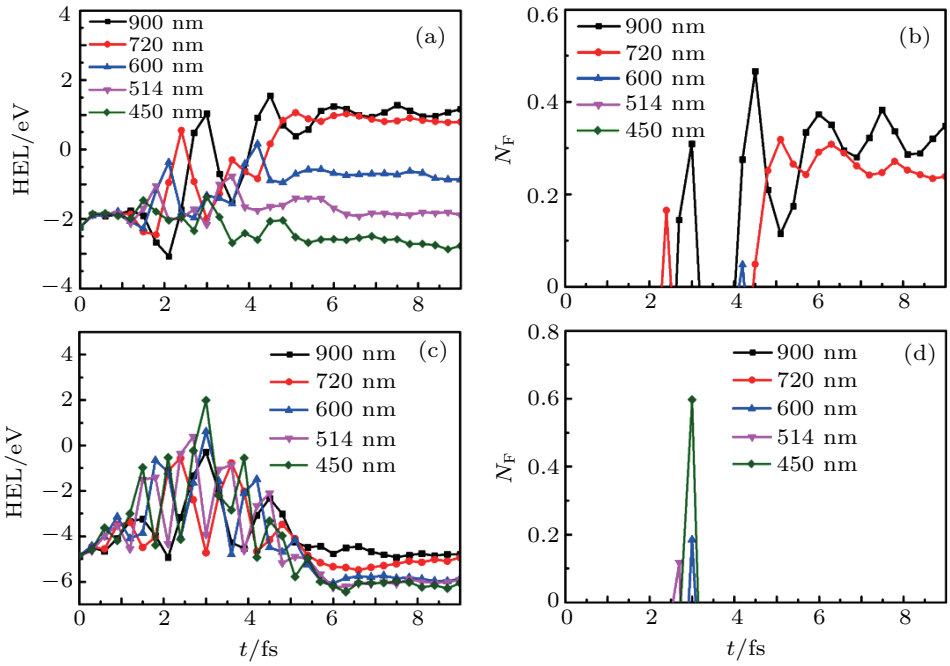


Fig. 7. (a) HEL and (b) N_F in PCTO-QDs, (c) HEL and (d) N_F in PCTO-QDs with intensity of incident ultrafast laser being 2.5 eV/Å for wavelengths of 450 nm, 514 nm, 600 nm, 720 nm, and 900 nm.

3.2.2. Influence of eigenfrequency and analysis

The unit conversion of 900 nm and 720 nm shows that the corresponding energy values are about 1.38 eV and 1.73 eV (see the inset in Fig. 8). It is concluded that this phenomenon is mainly caused by the fact that 900 nm and 720 nm are closer to the intrinsic frequency of PCTO-QDs, and thus making the optical carriers obtain higher resonance energy. The system obtains more power through coupling with the high frequency laser. It leads a metal area to break the bondage of insulator area, form light induced current. The electronic level collapse is discovered in laser pulses as the electronic oscillation can obtain more kinetic energy closer to the nuclear energy.[32] Next, for MCTO-QDs, this phenomenon is easy to understand. The shorter the laser wavelength, the higher the laser energy. And when the ability to bind the electrons is less than the laser energy, the HEL will cross the Fermi surface, thus it exhibits the metallic property.

By the way, we note a slightly difference in PCTO under the effect of the laser beam with a wavelength of 600 nm and a strength of 2.5 eV. This is because the incident direction of the laser in Fig. 4 is along the upper surface of the quantum dot, while the incident direction of the laser in Fig. 7 is along the center of the quantum dot. It can also confirm that the viewpoint of potential well mentioned in Subsubsection 3.1.2 is correct. When the plane of incidence hits along the center, the potential well turns deeper, the required energy increases, and we find that it is harder for the highest electron energy level to cross the Fermi plane. But its HEL trend is consistent with the laser waveform. This shows that our theoretical calculation results are reliable.

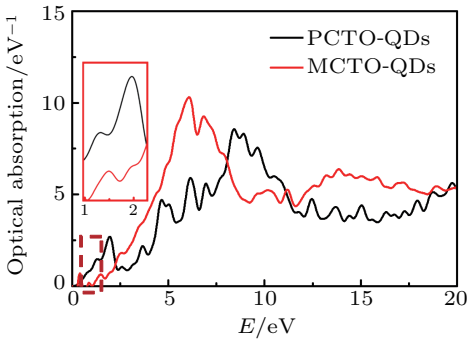


Fig. 8. Linear response (optical absorption) of PCTO-QDs (black) and MCTO-QDs (red).

4. Conclusions

In this work, we perform first-principles calculations to investigate the ultrafast laser interacting with PCTO-QDs and MCTO-QDs based on TDDFT. First, the effect of ultrafast laser on the final physical properties of the structure is directly related to whether the QD is modified. By controlling intensity, an insulator–metal transition is found, with the incident ultrafast laser irradiated. For PCTO-QDs, the physical property changing process is insulation–metal–insulation–metal. But for the MCTO-QDs, it experiences the process of insulation–metal–insulation, for which we conclude that there are three main reasons. One reason is that the unsaturated atoms around the unmodified quantum dots are more likely to absorb laser energy, and thus destroying the metallic properties of the structure. The second reason is that the modified quantum dot forms a potential well, and its geometric configuration can weaken the influence of laser energy. The third eason is that the structural damage caused by laser can affect its own nature to some extent. In addition, we also find that the frequency of the laser can also modulate the gold property of the quantum dot. We propose an idea that when the laser frequency is close to the present frequency of the quantum dot, it is easy to absorb the laser energy and produce changes. As the electronic oscillation can obtain more kinetic energy, the electronic level collapse is discovered. Our calculations provide the evidence to understand not only the insulator–metal transition but also the photoinduced dynamics of electrons in perovskite under laser.

References

[1] Grinberg I, West D V, Torres M, Gou G, Stein D M, Wu L, Chen G, Gallo E M, Akbashev A R and Davies P K 2013 *Nature* **503** 509

[2] Jeng J Y, Chiang Y F, Lee M H, Peng S R, Guo T F, Chen P and Wen T C 2013 *Adv. Mater.* **25** 3727

[3] Wang F, Grinberg I, Jiang L, Young S M, Davies P K and Rappe A M 2015 *Ferroelectrics* **483** 1

[4] Young S M and Rappe A M 2012 *Phys. Rev. Lett.* **109** 116601

[5] Veldhuis S A, Boix P P, Yantara N, Li M, Sum T C, Mathews N and Mhaisalkar S G 2016 *Adv. Mater.* **28** 6804

[6] Maeda K, Teramura K, Lu D, Takata T, Saito N, Inoue Y and Domen K 2006 *Nature* **440** 295

[7] Lee M M, Teuscher J, Miyasaka T, Murakami T N and Snaith H J 2012 *Science* **338** 643

[8] Kennedy C L, Hill A H, Massaro E S and Grumstrup E M 2017 *ACS Energy Lett.* **2** 1501

[9] Kabir I and Mahmood S 2019 *Chin. Phys. B* **28** 128801

[10] Zhang C, Sun D, Sheng C, Zhai Y, Mielczarek K, Zakhidov A and Vardeny Z 2015 *Nat. Phys.* **11** 427

[11] Leppert L, Reyes-Lillo S E and Neaton J B 2016 *J. Phys. Chem. Lett.* **7** 3683

[12] Miyano K, Tanaka T, Tomioka Y and Tokura Y 1997 *Phys. Rev. Lett.* **78** 4257

[13] Zhang Q, Su R, Du W, Liu X, Zhao L, Ha S T and Xiong Q 2017 *Small Methods* **1** 1700163

[14] Liu M, Hwang H Y, Tao H, Strikwerda A C, Fan K, Keiser G R, Sternbach A J, West K G, Kittiwatanakul S and Lu J 2012 *Nature* **487** 345

[15] Liu M, Pardo B, Zhang J, Qazilbash M, Yun S J, Fei Z, Shin J H, Kim H T, Basov D and Averitt R 2011 *Phys. Rev. Lett.* **107** 066403

[16] Kuzyk A, Pettersson M, Toppari J J, Hakala T K, Tikkanen H, Kunttu H and Törmä P 2007 *Opt. Express* **15** 9908

[17] Li Y J, Lv Y, Zou C L, Zhang W, Yao J and Zhao Y S 2016 *J. Am. Chem. Soc.* **138** 2122

[18] Hsu H L, Juang T Y, Chen C P, Hsieh C M, Yang C C, Huang C L and Jeng R J 2015 *Sol. Energy Mater. Sol. Cells* **140** 224

[19] Shamsi J, Dang Z, Bianchini P, Canale C, Di Stasio F, Brescia R, Prato M and Manna L 2016 *J. Am. Chem. Soc.* **138** 7240

[20] Sun S, Yuan D, Xu Y, Wang A and Deng Z 2016 *ACS Nano* **10** 3648

[21] Liu T, Zhang H and Cheng X 2019 *Opt. Express* **27** 16586

[22] Wang Y, Li X, Song J, Xiao L, Zeng H and Sun H 2015 *Adv. Mater.* **27** 7101

[23] Fonoberov V A and Balandin A A 2003 *J. Appl. Phys.* **94** 7178

[24] Kay H and Bailey P 1957 *Acta Crystallogr.* **10** 219

[25] Lemanov V, Sotnikov A, Smirnova E, Weihnacht M and Kunze R 1999 *Solid State Commun.* **110** 611

[26] Cockayne E and Burton B P 2000 *Phys. Rev. B* **62** 3735

[27] Marques M A, Castro A, Bertsch G F and Rubio A 2003 *Comput. Phys. Commun.* **151** 60

[28] Hartwigsen C, Gœdecker S and Hutter J 1998 *Phys. Rev. B* **58** 3641

[29] Delin A, Fast L, Johansson B, Eriksson O and Wills J 1998 *Phys. Rev. B* **58** 4345

[30] Šetrajčić J P, Armaković S, Šetrajčić I J and Džambas L D 2014 *Mod. Phys. Lett. B* **28** 1450023

[31] Anisimov S I, Kapeliovich B L, Perelman T L 1974 *Electron Emission from Metal Surfaces Exposed to Ultra-Short Laser Pulses [J]. Zhurnal Eksperimental'noi i Teroreticheskoi Fiziki* **66** 776

[32] Lin J H, Zhang H, Zhang B F, Zhao J, Miyamoto Y and Cheng X 2018 *J. Phys. Chem. C* **122** 19992

[33] Goul R, Das S, Liu Q, Xin M, Lu R, Hui R and Wu J Z 2017 *Carbon* **111** 386

[34] Knorr I, Christou K, Meinertz J, Selle A, Ihlemann J and Marowsky G 2008 *COMSOL Conference* pp. 1–7